17th International Conference on
AEROSPACE SCIENCES & AVIATION TECHNOLOGY,
ASAT - 17 – April 11 - 13, 2017, E-Mail: asat@mtc.edu.eg
Military Technical College, Kobry Elkobbah, Cairo, Egypt
Tel: +(202) 24025292 – 24036138, Fax: +(202) 22621908

Effect of Prestressing Multilayer Steel Armor on Its Impact Resistance to Blunt Rigid Projectiles

S. A. K. Yossif*

Abstract: This paper investigates numerically the enhancement of impact resistance of multiplayer steel armor to rigid and blunt projectiles. The monolithic armor always possesses higher ballistic resistance than the multilayer one of the same weight and areal density. In this work, the monolithic Weldox 460E steel armor is divided into three layers. The front and rear layers have the same thickness and they are thinner than the middle one. The thicker middle layer is prestressed by applying initial compressive strain. Then, the yield point of the middle layer is raised and the overall impact resistance of the prestressed multilayer armor is increased. The prestressed armor is impacted by a high-speed armor piercing (AP) blunt and rigid projectile. The impact resistance is macroscopically measured as the percentage reduction in the kinetic energy (KE) of the AP projectile. The percentage reductions in KE are calculated for the monolithic armor, equal and different thicknesses three layers armors with and without prestressing their middle layers. According to the presented computations, the maximum reduction in KE corresponds to the different thickness three layers armor having its thicker middle layer been prestressed.

Keywords: Impact resistance, multilayer armor, armor piercing projectile prestressing, Weldox steel armor, numerical simulation, finite element method.

1. Introduction

Ballistic characteristics of monolithic and multilayers armors attract the attention of many researchers. M.A. Abdel-Wahed et al [1] studied the ballistic resistance of monolithic and layered steel armors. The layered armors were in double and triple layers both in contact and spaced by air gaps. The armors were shot by armor piercing (AP) projectiles with the caliber of $7.62\,mm$. The impact velocities were ranging from $300\,m/s$ to $600\,m/s$. The total thicknesses of the layered and monolithic armors were the same and equal to $3\,mm$. They performed both experimental and numerical simulation work. They reached to the following two important conclusions. Firstly, the single layer armor has the greatest ballistic resistance except at impact velocity of $558\,m\,/\,s$ where the in-contact triple layers target becomes the best. Secondly, at the high impact velocities both double and triple layers targets have the same impact resistance. The same conclusions were drawn by A.M. Eleiche et al [2]. X. Teng et al [3] used the finite element method (FEM) to estimate the protection performance of double-layered shields against projectiles impacted at the sub-ordnance velocity. The projectiles had flat-nose (blunt) and conical nose ends. The shields were made of Weldox 460E steel having a total thickness of $12\,mm$. The double-layered shields were in contact and

* Lecturer at Mechanical Design Department - Faculty of Engineering – Materia - Helwan University – Cairo – Egypt; salah.aleasha@hotmail.com

separated by an 3 mm air gap. The authors found that the double-layered configuration is able to improve the ballistic performance in case of flat-nose projectiles, when compared to the monolithic plate having the same weight. However, in case of conical-nose projectile, the performances of double-layered and monolithic shields are the same. V. Madhu et al [4] studied experimentally the impact of hard steel AP projectiles on mild steel and aluminum targets. The target's configurations were single and layered plates. They concluded that the residual velocities in case of intermediate thickness double layered mild steel plates were as the same order as the monolithic one.

The present work aims to enhance the impact resistance of multilayer steel armors. It is proposed to prestress the interlayer of the armor. The prestressed layer should be thick enough to avoid the risk of buckling. For simplicity, the present paper investigates three layers armor. This study includes the following sections: description of computational models, material modeling, implementation of initial prestressing, discussion of simulation results and conclusion. All numerical simulations are performed by the commercial finite element program ABAQUS/Explicit.

2. Monolithic and Multilayered Armor Computational Models

The computational model of a monolithic armor is illustrated in Fig. 1(a). The armor is made of Weldox 460E steel. It is a disc of diameter $\emptyset 100\ mm$ and thickenss of $12\ mm$. The rigid and blunt AP projectile has diameter of $\emptyset 7.6\ mm$ and length of $30\ mm$. The mass of AP projectile (bullet) is selected to be $10\ g$. The projectile has initial impact velocity of $V_o = 600\ m/s$. This high velocity is intentionally selected to ensure complete penetration and perforation of the armor either monolithic or multilayered. As the projectile leaves the armor, its velocity is denoted by V_r. The reduction in kinetic energy of AP projectile is selected to macroscopically measure the impact resistance of the armor. Since the projectile is rigid, the percentage reduction in its kinetic energy ΔKE is calculated as the following:

$$\Delta KE = \frac{V_o^2 - V_r^2}{V_o^2} \times 100\ \% \qquad (1)$$

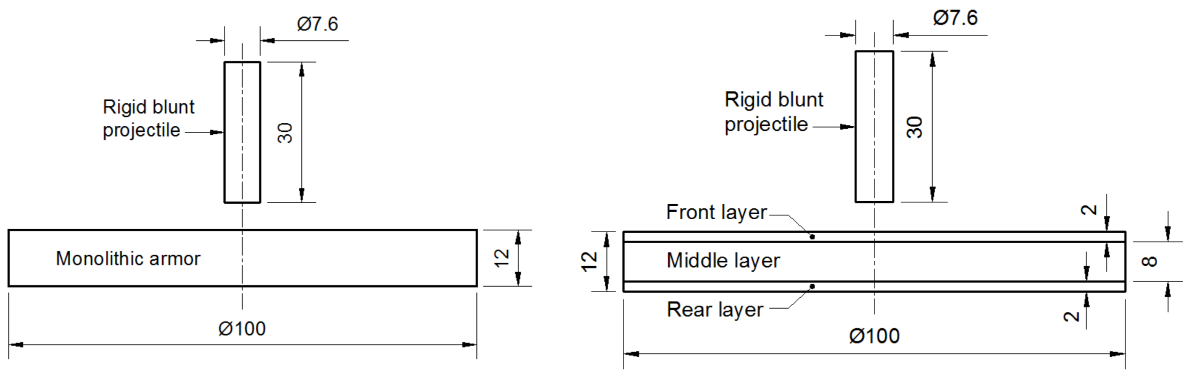

(a) (b)

Fig. 1. Computational Models; (a) Monolithic Armor and (b) Triple Layers Armor. Dimensions are in mm.

Frictionless contact is assumed between the projectile and the target; Fig. 2(a). This assumption is reasonable because the contact between the rigid bullet and the deformable armor occurs at very high speed and lasts very short duration of time.

Due to the symmetry of the problem, the two-dimensional axisymmetric finite element model is recommended, Fig. 2(a). The left edges of the bullet and armor are symmetric while the right edge of the armor is clamped. The armor is meshed using four nodes axisymmetric reduced integration ABAQUS element (CAX4R). Number of elements and nodes are 6000 and 6161 respectively, Fig. 3(a). The mesh density increases gradually towards the center of armor where the impact occurs.

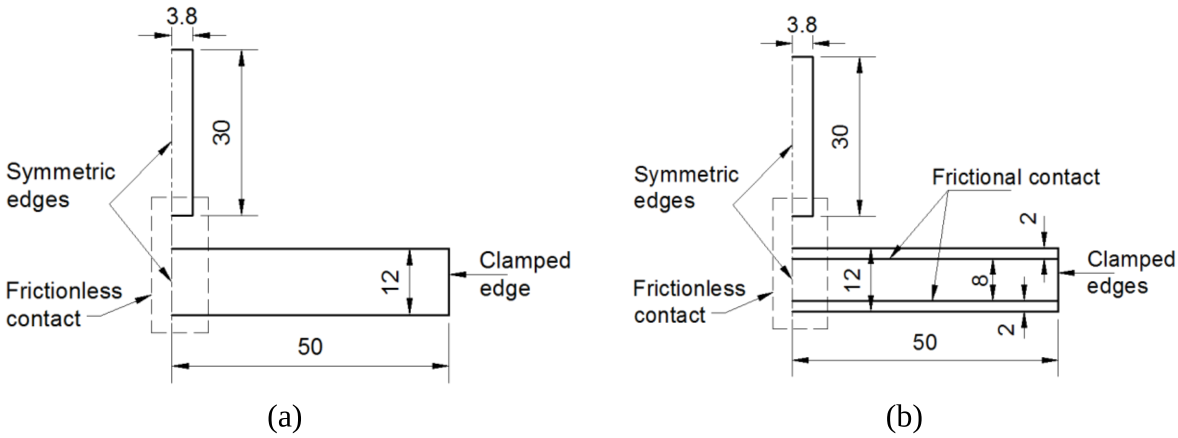

Fig. 2. Symmetric Models; (a) Monolithic Armor and (b) Triple Layers Armor. Dimensions are in mm.

Figure 1(b) illustrates the computational model for the triple layers armor. The thickness of the monolithic armor is divided into three layers; front, middle and rear. The layers thickness are $2\,mm$, $8\,mm$ and $2\,mm$ respectively. The overall thickness and material of the monolithic and the layered armors are kept the same for comparison purposes. The middle layer is made thicker to avoid the risk of buckling, as the layer receives an initial compressive strain. Surfaces of the three layers are in frictional contact, Fig. 2(b). The coefficient of friction is selected to be 0.1. The contact between the rigid projectile and the three deformable layers is assumed to be frictionless, Fig. 2(b). Such assumption is based on the nature of the contact where its duration is very short and speed is very high. The symmetric model of the triple layers armor is shown in Fig. 2(b). The triple layers armor is meshed by 6002 elements of type (CAX4R) having 6364 nodes, Fig. 3(b). The mesh morphology of the layered armor is identical as possible to that of monolithic armor for comparison purposes, Fig. 3.

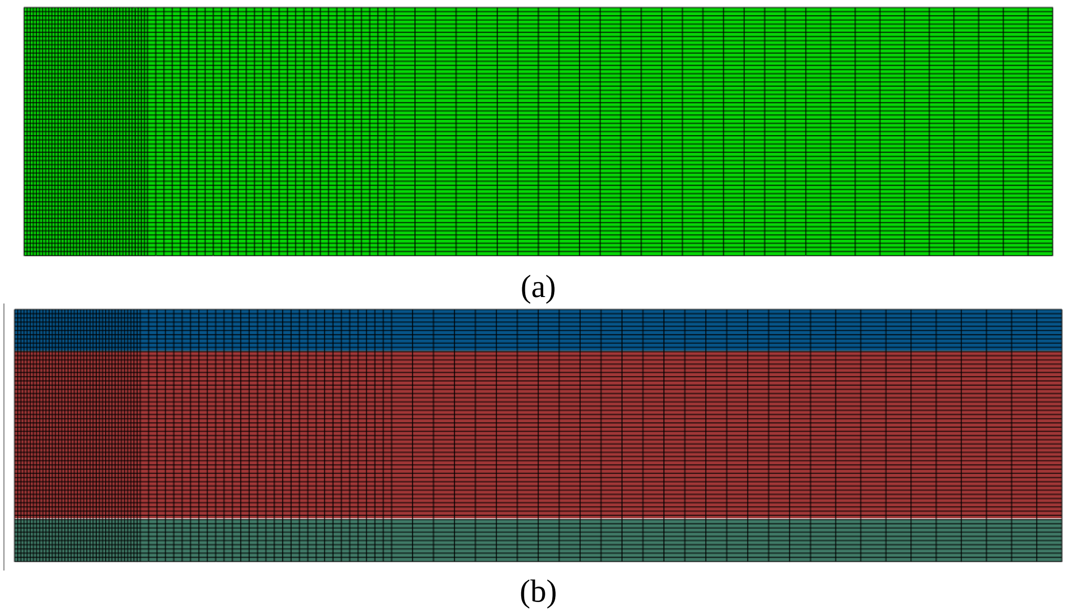

Fig. 3. Finite Element Models; (a) Monolithic Armor and (b) Triple Layers Armor.

3. Material Modeling

The plastic and fracture behaviors of Weldox 460E steel are simulated using the Johnson-Cook (JC) plasticity and dynamic fracture models [3]. Both models are implemented in ABAQUS/Explicit [5]. The JC plasticity model is a particular type of Mises plasticity model. It considers isotropic hardening, strain-rate and temperature dependences of the yield stress. The mathematical form of JC plasticity model is [5]:

$$\sigma = \left[A + B\bar{\varepsilon}_{pl}^{n}\right]\left[1 + C\ln\left(\frac{\dot{\bar{\varepsilon}}_{pl}}{\dot{\bar{\varepsilon}}_{o}}\right)\right]\left[1 - \hat{T}^{m}\right] \quad (2)$$

where σ is the yield stress, $\bar{\varepsilon}_{pl}$ is the equivalent (effective) plastic strain, A, B, C, n and m are material constants, $\dot{\bar{\varepsilon}}_{pl}$ is current plastic strain, $\dot{\bar{\varepsilon}}_{o}$ is reference strain, $\hat{T}$ is the homologous temperature defines as the following:

$$\hat{T} = \begin{cases} 0 & for \quad T < T_o \\ \frac{T - T_o}{T_m - T_o} & for\ T_o \le T \le T_m \\ 1 & for \quad T > T_m \end{cases} \quad (3)$$

where T is the current temperature, T_m is melting temperature, T_o is the transition temperature defined as the one at or below which there is no temperature dependence of the yield stress. The JC dynamic fracture model depends on the calculation of a damage parameter ω for each element. If $\omega \ge 1$, the element is considered as damaged and removed from the subsequent computations. The expression of the damage parameter is [5]:

$$\omega = \sum \frac{\Delta\bar{\varepsilon}_{pl}}{\varepsilon_f} \quad (4)$$

where $\Delta\bar{\varepsilon}_{pl}$ is an increment of the equivalent plastic strain, and ε_f is the strain at failure. The failure strain is calculated according to the following equation [5]:

$$\varepsilon_f = \left[D_1 + D_2 \exp\left(D_3 \frac{\sigma_m}{q}\right)\right]\left[1 + D_4 \ln\left(\frac{\dot{\bar{\varepsilon}}_{pl}}{\dot{\bar{\varepsilon}}_{o}}\right)\right]\left[1 + D_5\hat{T}\right] \quad (5)$$

where constants D_1 to D_5 are damage parameters, σ_m is the mean stress, and q is the von Mises stress.

According to the experimental work of Borvik et al [3], the material constants and damage parameters for Weldox 460E steel are listed in Table 1.

Table 1. Material Constants and Damage Parameters for Weldox 460E steel [3].

Constants	Value	Unit
A	490	MPa
B	383	MPa
n	0.45	
m	0.94	
C	0.00123	
$\dot{\bar{\varepsilon}}_{o}$	0.0005	$1/s$
T_o	293	K
T_m	1800	K

Constants	Value	Unit
ρ	7850	Kg/m^3
E	200	GPa
ν	0.33	
D_1	0.0705	
D_2	1.732	
D_3	-0.54	
D_4	0	
D_5	0	

4. Implementation of Initial Prestress

The layers of the prestressed armor should be enclosed in a rigid frame. The diameter of the middle layer should be larger than that of the other front and rear layers. Figure 4(a) illustrates the dimensions, stress and strain states of the middle layer before the prestressing process. The diameter of the layer was $102\ mm$ and its thickness was $8\ mm$. The yield point of layer's material was $490\ MPa$. The middle layer is shrunk into the rigid frame. The layer is subjected to a radial displacement of $u_r = 1\ mm$, as shown in Fig. 4(b). After, the shrink-fit process, the diameter of the middle layer becomes $\phi 100\ mm$ which is equal to that of the other layers. As a consequence of prestressing process, plastic deformation of $\varepsilon_{pl} = 0.00355$ is developed in the layer. This residual plastic deformation rises the yield point of layer's material from $490\ MPa$ to $605.5\ MPa$, Fig. 4(b). This increase in the yield point of the middle layer will enhance its impact resistance to the penetration of the AP rigid bullet.

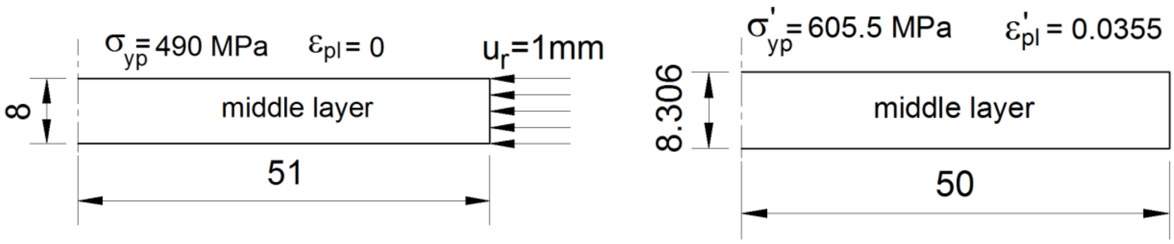

(a) (b)

Fig. 4. Middle Layer; (a) Before and (b) After Initial Prestressing Process.

In this work, the process of prestressing is considered as a static step. This static step is followed by an explicit dynamic step that simulates the impact of the bullet to the prestressed armor. The increase in the thickness of the middle layer due to prestressing, Fig. 4(b), is considered in the second explicit dynamic simulation step.

5. Discussion of Simulation Results

Figure 5 illustrates impact, penetration and perforation stages of the monolithic armor by the AP blunt projectile. During the first microseconds of the impact, the high speed rigid blunt projectile presses down the material of the front surface of the armor, Fig. 5(a). A small petal of pushed away material appears on the front surface of the armor having a diameter larger than that of the bullet. In addition, a concave cavity appears around the rigid boundaries of the projectile, Fig. 5(a). As the bullet penetrates into the armor, it plastically shears its material. Armor' material flows plastically on the flat nose surface and on the rigid boundaries of the projectile. Consequently, the concave cavity disappears and the diameter of the penetrated material becomes equal to that of the bullet, Fig. 5(b). Finally, the projectile completely perforates the armor, Fig. 5(c). A thin layer of armor material is plugged off – a process called shear plugging. Time history of projectile's velocity is plotted in Fig. 7. The projectile exits from the armor by a residual velocity $V_r = 269.22 \frac{m}{s}$, Table 2 and Fig. 7. This value of residual velocity is compared with that was published in [3] ($|V_r|_{[3]} = 276 \frac{m}{s}$ Figure 17). The percentage error in residual velocity is $-2.46\ \%$, which is very small to give reasonable confidence of the present computations. The negative sign of AP's velocity appears in Fig. 7 is due to that the direction of AP projectile motion opposes that of global y coordinate. The percentage reduction in kinetic energy of the projectile piercing the monolithic armor is 79.87%, Table 2.

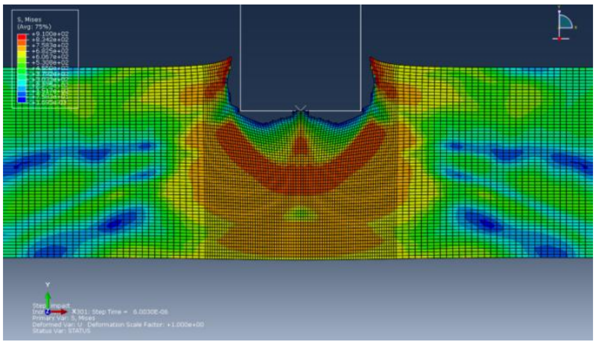

(a) $time = 6\ \mu s$

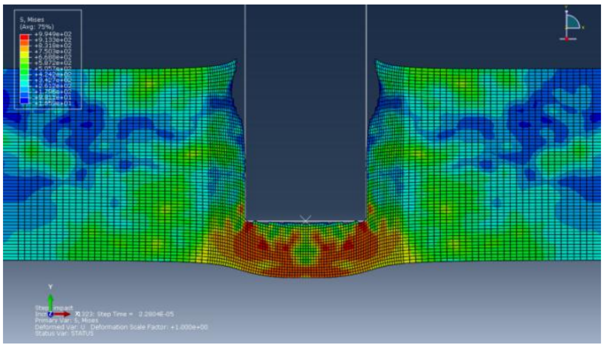

(b) $time = 22.8\ \mu s$

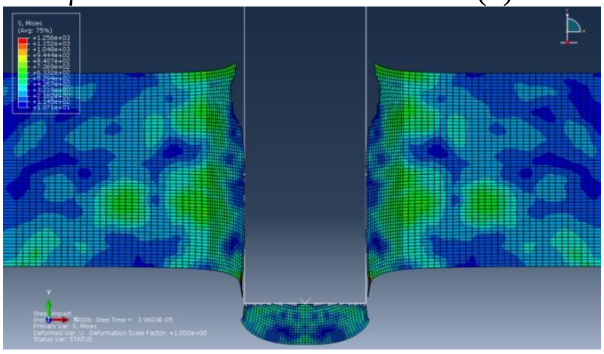

(c) $time = 39.6\ \mu s$

Fig. 5. Impact of Monolithic Armor by a Rigid Blunt Projectile.

Figure 6 illustrates the dynamic behavior of three layers different thicknesses armor having its middle layer was initially prestressed. The prestressed triple layers armor is impacted by AP blunt projectile. The thin front layer exhibits small petal on its surface and shallow concave cavity around the rigid projectile, Fig. 6(a). Due to the high impulse, layers of the armor start to lose their initial contact. The maximum separation is found to be between the middle and the rear layers as the bullet completely perforates the armor, Fig. 6(c).

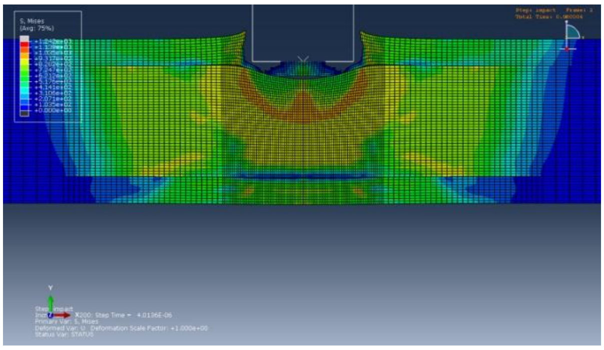

(a) $time = 4\ \mu s$

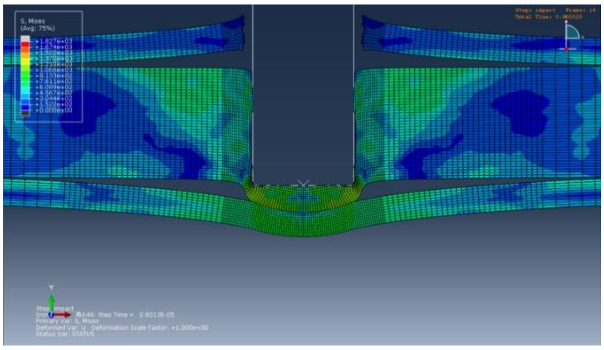

(b) $time = 28\ \mu s$

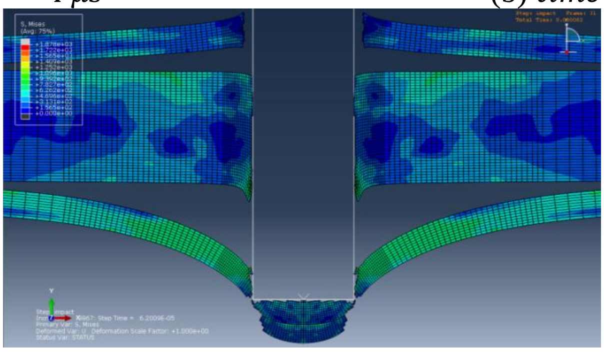

(c) $time = 62\ \mu s$

Fig. 6. Impact of Three Layers Prestressed Armor by a Rigid Blunt Projectile.

The initial rise in the yield point of the prestressed middle layer, Fig. 4(b), prevents the formation of neither small petals nor concave cavities as the projectile penetrates the layer, Fig. 6(b). This is a symptom to the noticeable increase in the layer resistance to plastic deformation. This local increase in middle layer resistance leads to the overall enhancement of impact resistance of the prestressed armor. However, the initial prestressing didn't influence on the process of shear plugging and a metal plug is formed, Fig. 6(b). Small inverted crater was formed in the back surface of the middle layer, where the material was plugged off, Fig. 6(c). Both projectile and the plugged material from the middle layer impact the thin rear layer. The layer is perforated and severely bent downwards, Fig. 6(c). The petal on the top surface of the rear layer is completely destroyed. The rear layer continuously loses its contact with the middle one. Two layers of plugged material are detached, as the armor's structure is layered one, Fig. 6(c). The residual velocity of the projectile as it exits from the prestressed three layers armor is $V_r = 221.15\frac{m}{s}$, Table 2 and Fig. 7. The corresponding percentage reduction in kinetic energy of the projectile is 86.41%, Table 2.

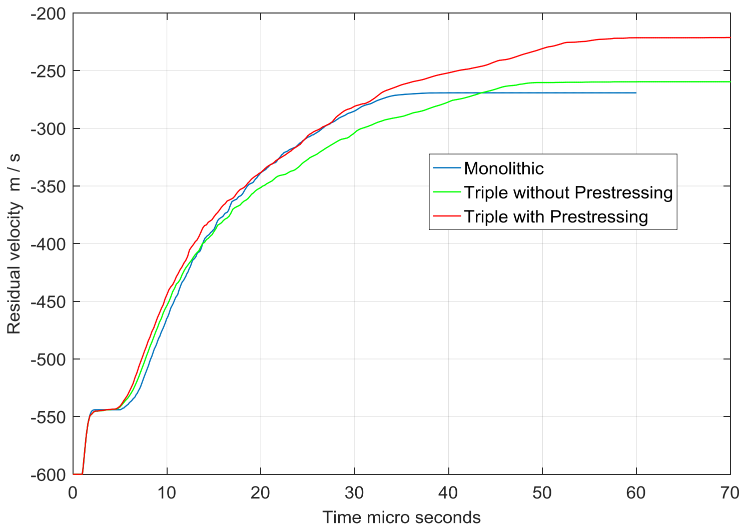

Fig. 7. Residual Velocities of Projectile Related to Monolithic and Three Layers Armor with and without Initial Prestressing.

It is worthy to investigate the dynamic behavior of the different thickness three layers armor without prestressing its middle layer. This enables the researcher to probe the effect of initial prestressing only. The time history of the projectile's velocity impacting the triple layer armor without prestressing is plotted in Fig. 7. The value of bullet's speed as it leaves the armor is found to be $V_r = 259.6\frac{m}{s}$, Table 2. The reduction in kinetic energy in case of triple armor without prestressing is 81.28 %, Table 2.

Table 2. Residual Velocities and Percentage Reduction in Projectile Kinetic Energies in Case of Monolithic and Three Layers Armor with and without Initial Prestressing.

Armor	Residual Velocity, [m/s]	Percentage Reduction in Kinetic Energy, [%]
Monolithic	269.22	79.87%
Three layers without prestressing	259.6	81.28%
Three layers with initial prestressing.	221.15	86.41%

By inspection of Fig. 7 and Table 2, it is found that the impact resistance of different thickness triple armor without initial prestressing in higher than that is in the case of monolithic armor. However, the impact resistance of different thickness three layers armor, whose thicker middle layer was initially prestressed, is the highest.

6. Conclusion

It is proved numerically that initial prestressing of the middle layer in different thicknesses layered armor may increase armor's impact resistance to blunt projectiles.

7. References

[1] M.A. Abdel-Wahed, A.M. Salem, A.S. Zidan and A.M. Riad, "Penetration of a Small Caliber Projectile into Single and Multi-layered Targets", EPJ Web of Conferences, 6, 02004, 2010. http://dx.doi.org/10.1051/epjconf/20100602004
[2] A.M. Eleiche, M.S. Abdel-Kader, A. Almohandes, "Penetration Resistance of Laminated Plates From Steel and Fiberglass-Reinforced Polyester", Transactions on the Built Environment, Vol. 22, 1996.
[3] Xiaoqing Teng, Sumita Dey, Tore Børvik and Tomasz Wierzbicki, "Protection Performance of Double-Layered Metal Shields Against Projectile Impact", Journal of Mechanics of Materials and Structures, Vol. 2, No. 7, 2007.
[4] V. Madhu, T. Balakrishna Bhat, and N.K. Gupta, "Normal and Oblique Impacts of Hard Projectile on Single and Layered Plates - An Experimental Study", Defence Science, Vol. 53, No. 2. April 2003, pp. 147-156.
[5] ABAQUS Documentation, Dassault Systèmes, 2015.